ChemComm

COMMUNICATION

View Article Online
View Journal | View Issue

Cite this: *Chem. Commun.*, 2025, **61**, 8883

Received 10th March 2025,
Accepted 7th May 2025

DOI: 10.1039/d5cc01306b

rsc.li/chemcomm

Tailoring the properties of guaiacol-derived high sulfur-content materials through post-polymerization modification with dithiols†

Nawoda L. Kapuge Dona,[a] Rhett C. Smith *[a] and Andrew G. Tennyson *[ab]

High sulfur content material (HSM) prepared from biomass-derived guaiacol and elemental sulfur (GS_{80}) was modified with dithiols at varying mass ratios. Dithiol modification allowed tuning of the material properties, such as a predictable relationship between glass transition temperature and proportion of added dithiol. Dithiol modification is thus a promising new strategy for customized HSMs.

High sulfur content materials (HSMs) are gaining significant attention in various fields due to their unique chemical and physical properties.[1–6] HSMs are often prepared by inverse vulcanization, the reaction of majority component elemental sulfur with organics,[7–16] and comprise sulfur catenate-crosslinked materials (Scheme 1). Many sustainable organics have been utilized to prepare HSMs, including biomass compounds,[17–21] animal fats,[22–25] plant oils,[26–39] and lignin derivatives such as **GS_{80}**, a composite prepared from 80 wt% sulfur and 20 wt% guaiacol (Scheme 1).[40–45]

Recent work has amplified the versatility of post-vulcanization modification for tuning the properties of HSMs. For example, improvements in mechanical strength/strain profiles can be achieved by adding polybutadiene to HSM formulations,[46] by post-vulcanization crosslinking *via* added an epoxide-bearing monomer,[47] by changing the reaction temperature to induce cyclization/aromatization of terpene monomers,[48,49] or *via* a two-stage sequential crosslinking approach.[50]

The mechanical properties of vulcanized rubber have been similarly enhanced by incorporating crosslinkers such as thiazoles, sulfenamides, thioureas, polycysteine and dithiols.[51–54] We hypothesized that dithiols could also be used to effect the post-vulcanization property tuning of HSMs. To test this hypothesis, **GS_{80}** (prepared from 20 wt% guaiacol and 80 wt% sulfur)[43] was treated with dithiols in various mass ratios followed by spectroscopic, thermal, and mechanical analysis. Dithiols were expected to insert into flexible sulfur catenates in **GS_{80}** as shown in Scheme 1, so it was reasoned that incorporating rigid segments would elicit the greatest change in properties. Moreover, aryl thiols generally exhibit low homolytic S–H bond dissociation energies compared to alkyl analogues, further facilitating desired reactivity.[55] Rigid benzene-1,4-dithiol (BDT) and 4,4′-biphenyldithiol (BPDT) were thus selected for the initial study. Each dithiol was heated with **GS_{80}** in **GS_{80}**:dithiol mass ratios of 2 : 1, 3 : 1, 4 : 1, 5 : 1, and 10 : 1 at 180 °C for 1 h under N_2 in sealed pressure tubes. Upon cooling to room temperature, all the products formed were remeltable and ranged from light brown to nearly black color.

The Fourier-transform infrared (FT-IR) spectra of dithiol-crosslinked composites (Fig. S1–S14, ESI†) provide evidence for dithiol insertion through the disappearance of the S–H stretching peak at 2549 cm^{-1} (Fig. S1 and S8, ESI†). The relative intensity of the dithiol aromatic ring mode band (1473 cm^{-1} for both BDT and

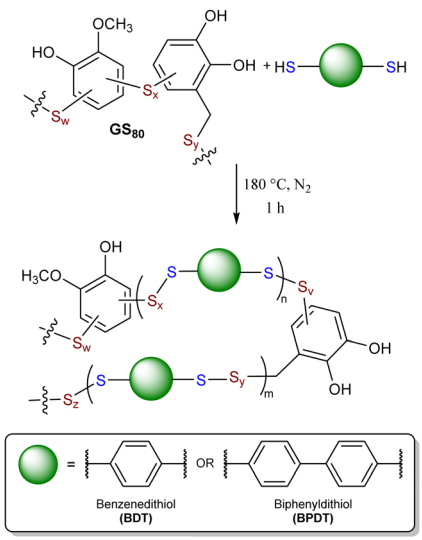

Scheme 1 A proposed reaction pathway for modifying **GS_{80}** with benzene-1,4-dithiol (BDT) or 4,4′-biphenyldithiol (BPDT).

[a] *Department of Chemistry, Clemson University, Clemson, South Carolina, 29634, USA. E-mail: rhett@clemson.edu*
[b] *Department of Materials Science and Engineering, Clemson University, Clemson, South Carolina, 29634, USA. E-mail: atennys@clemson.edu*

† Electronic supplementary information (ESI) available: FT-IR spectra, TGA curves, DTG curves and DSC curves. See DOI: https://doi.org/10.1039/d5cc01306b

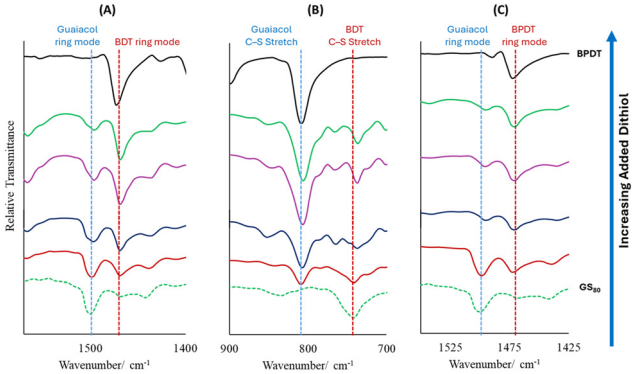

Fig. 1 Infrared spectra show that progressive addition of dithiol is accompanied by proportional increases in the relative intensity of dithiol-derived bands including (A) the aromatic ring mode of BDT *versus* that of the guaiacol rings of **GS$_{80}$**, (B) the C–S bond stretch mode of BDT *versus* that of **GS$_{80}$**, and (C) the aromatic ring mode of BPDT *versus* that of the guaiacol rings in **GS$_{80}$**. These trends are accompanied by the disappearance of the band attributable to dithiol S–H stretches (Fig. S1 and S8 in the ESI†).

BPDT) relative to that in **GS$_{80}$** (1500 cm^{-1}) progressively increased with added BDT (Fig. 1A) or BPDT (Fig. 1C). In the case of BDT-modified **GS$_{80}$**, well-resolved C–S stretches were observed attributable to C–S bonds to guaiacol in **GS$_{80}$** (740 cm^{-1}) and to benzene in BDT (802 cm^{-1}), with a progressive increase in relative intensity of the BDT C–S stretch with increasing BDT addition (Fig. 1B). These spectral features indicate complete consumption of thiol S–H bonds with retention of the –S–Ar–S– units.

Scanning electron micrographs (SEM) with element mapping by energy dispersive X-ray analysis (EDX) (Fig. S29 and S30, ESI†) also confirmed the homogeneity of the materials with a uniform distribution of sulfur, carbon, and oxygen across all samples.

Whereas EDX data reveal uniform distribution of sulfur in the materials, the sulfur in the HSMs generally exists in two forms: (a) as oligo/polysulfide chains that are covalently attached to organic species *via* C–S bonds, and (b) as physically entrapped oligosulfur species within the polymer network, here collectively referred to as ''dark sulfur''.[56] Because dark sulfur is not covalently bound to the crosslinked network solid, it can be effectively extracted and quantified using a UV-vis method developed by Hasell *et al.*[57] All of the S–S bonds in **GS$_{80}$** – whether covalently anchored to organics or in dark sulfur – are susceptible to reaction with dithiols, so as progressively more dithiol is added, concomitantly less extractable sulfur is anticipated. This general trend was observed (Table 1) for BDT-modified materials, with dark sulfur decreasing from 23 wt% in unmodified **GS$_{80}$** to 1 ± 3 wt%, as well as in BPDT-modified materials, with dark sulfur again decreasing from 23 wt% in unmodified **GS$_{80}$** to 2 ± 3 wt%. These data provide further evidence for the anticipated chemistry.

The thermal properties of the composites were analysed using thermogravimetry analysis (TGA; TGA and DTG curves are provided in Fig. S15–S18, ESI†). The decomposition temperatures (T_d, provided as the local maximum of the derivative TGA curve, corresponding to the maximum rate of mass loss) are summarized in Table 1. For **GS$_{80}$**-BDT-modified composites, the major decomposition was observed at 272–333 °C (0–33.3 wt% of BDT), attributed to the sublimation of sulfur from the material. In contrast, BPDT-modified materials having low amounts of added BPDT showed an initial minor decomposition at 99–114 °C and a major decomposition of the BPDT-modified composites at 272–329 °C due to the sublimation of sulfur. The T_d values for the main decomposition event increased progressively with higher weight percentages of added dithiol, consistent with the expected progressively shorter and more stable sulfur catenates. BDT-modified composites generally exhibited slightly higher decomposition temperatures than BPDT-modified composites. A minor decomposition event at a higher temperature (>348 °C) attributable to the decomposition of aryl organosulfur species was discerned for materials made with higher amounts of added aryl thiol. The increase in char yield followed a predictable trend, correlating with a higher proportion of dithiol content (Fig. 2A), consistent with the increased aryl content in the materials.

Differential scanning calorimetry (DSC; full traces shown in Fig. S19–S28, ESI†) analysis from −60 °C to 140 °C revealed a progressive increase in the glass transition temperature (T_g) with increasing addition of rigid dithiols (Fig. 2B). The trend in T_g values shown in Fig. 2B highlights a relationship between incorporated dithiol and glass transition temperature (T_g), which spans the range from −34 °C to 6 °C for BDT-modified materials and −34 °C to 14 °C for BPDT-modified materials, offering a wide range of tunability. For a given ratio, BPDT-modified materials exhibited higher T_g values compared to BDT-modified materials, attributable to the longer rigid spacer in biphenyl *versus* phenyl moieties.

Shore A hardness is a common assessment of hardness for factices, HSMs, and post-vulcanization-modified rubber.[47,58–61]

Table 1 Thermo-morphological properties and Shore A hardness measurements for dithiol-modified GS$_{80}$ products compared to unmodified GS$_{80}$

	T_d[a]/°C		Char yield[b] (wt%)		$T_{g,DSC}$[c]/°C		Dark sulfur (wt%)[d]		Shore A hardness/HA	
Material	BDT	BPDT	BDT	BPDT	BDT	BPDT	BDT	BPDT	BDT	BPDT
GS$_{80}$-dithiol (2 : 1)	333	329	20	27	6	6	6 ± 3	2 ± 3	53	74
GS$_{80}$-dithiol (3 : 1)	328	323	16	19	4	4	1 ± 3	11 ± 3	62	92
GS$_{80}$-dithiol (4 : 1)	320	321	11	16	−6	−6	13 ± 3	17 ± 3	60	89
GS$_{80}$-dithiol (5 : 1)	312	316	11	13	−6	−7	22 ± 3	16 ± 3	74	87
GS$_{80}$-dithiol (10 : 1)	311	313	5	5	−16	−21	22 ± 3	14 ± 3	75	82
GS$_{80}$[e]	272		0		−34		23		85	

[a] The local maximum temperature of the major mass loss by the TGA derivative curve. [b] The residue remaining at the end of TGA at 800 °C (directly taken from the TGA curve). [c] Glass transition temperature. [d] Percent ethyl acetate-extractable sulfur species. [e] **GS$_{80}$** was prepared from 80 wt% sulfur and 20 wt% guaiacol.

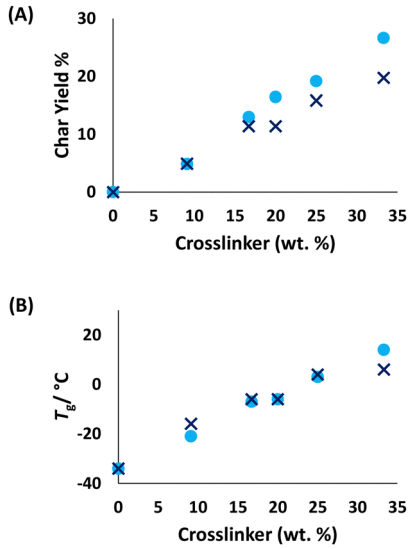

Fig. 2 Graphical representation of the general trend showing the effect of increasing the percentage of BDT (dark blue) and BPDT (light blue) dithiol crosslinkers on (A) char yield% and (B) glass transition temperature (T_g).

Shore A hardness measurements (Table 1) show substantial variability in hardness from parent $\mathbf{GS_{80}}$ (85 A) to BDT-modified materials 53–75 A, and BPDT-modified systems range from 74–92 A. These values do not follow a predictable trend. Overall, the hardness of these materials falls within the range for soft rubbers, synthetic resins and semirigid plastics, which are commonly used in commercial items such as pencil erasers (50 A), shoe heels (70 A), leather belts (80 A), tire treads (70 A) and shopping cart wheels (90 A).[62,63] Reproducibility in Shore A hardness values across multiple positions within the samples indicates effective diffusion and uniform incorporation of dithiols on a macroscale.

In conclusion, this study demonstrates that post-vulcanization modification of $\mathbf{GS_{80}}$ with rigid dithiols is an effective strategy for tuning the properties of high sulfur-content materials. The incorporation of benzene-1,4-dithiol (BDT) and 4,4′-biphenyldithiol (BPDT) not only facilitated the predictable increase in glass transition temperature but also reduced the extractable "dark sulfur" content. Thermal and mechanical evaluations further revealed enhanced decomposition profiles and tailored hardness properties. These findings underscore the potential of dithiol crosslinking to customize HSMs for diverse applications, paving the way for further exploration of post-vulcanization strategies in advanced material design.

We thank the National Science Foundation (CHE-2203669 to RCS) for financial support.

Data availability

The data supporting this article have been included as part of the ESI.†

Conflicts of interest

There are no conflicts to declare.

Notes and references

1 A. Nayeem, M. F. Ali and J. H. Shariffuddin, *Environ. Res.*, 2023, **216**, 114306.
2 A. Nayeem, M. F. Ali and J. H. Shariffuddin, *Mater. Today: Proc.*, 2022, **57**, 1095–1100.
3 A. Amin, N. M. Mahmoud and Y. W. Z. Nisa, *Green Mater.*, 2020, **8**, 172–180.
4 J. M. Chalker, M. J. H. Worthington, N. A. Lundquist and L. J. Esdaile, in *Sulfur Chemistry*, ed. X. Jiang, Springer International Publishing, Cham, 2019, pp. 125–151, DOI: 10.1007/978-3-030-25598-5_4.
5 F. Zhao, Y. Li and W. Feng, *Small Methods*, 2018, **2**, 1–34.
6 D. A. Boyd, *Angew. Chem., Int. Ed.*, 2016, **55**, 15486–15502.
7 W. J. Chung, J. J. Griebel, E. T. Kim, H. Yoon, A. G. Simmonds, H. J. Ji, P. T. Dirlam, R. S. Glass, J. J. Wie, N. A. Nguyen, B. W. Guralnick, J. Park, Á. Somogyi, P. Theato, M. E. Mackay, Y.-E. Sung, K. Char and J. Pyun, *Nat. Chem.*, 2013, **5**, 518–524.
8 C. M. Marshall, J. Molineux, K.-S. Kang, V. Kumirov, K.-J. Kim, R. A. Norwood, J. T. Njardarson and J. Pyun, *J. Am. Chem. Soc.*, 2024, **146**, 24061–24074.
9 J. Lim, J. Pyun and K. Char, *Angew. Chem., Int. Ed.*, 2015, **54**, 3249–3258.
10 J. J. Griebel, G. Li, R. S. Glass, K. Char and J. Pyun, *J. Polym. Sci., Part A: Polym. Chem.*, 2015, **53**, 173–177.
11 I. Gomez, D. Mecerreyes, J. A. Blazquez, O. Leonet, H. Ben Youcef, C. Li, J. L. Gomez-Camer, O. Bundarchuk and L. Rodriguez-Martinez, *J. Power Sources*, 2016, **329**, 72–78.
12 I. Gomez, A. F. De Anastro, O. Leonet, J. A. Blazquez, H.-J. Grande, J. Pyun and D. Mecerreyes, *Macromol. Rapid Commun.*, 2018, **39**, 1800529.
13 J. A. Smith, S. J. Green, S. Petcher, D. J. Parker, B. Zhang, M. J. H. Worthington, X. Wu, C. A. Kelly, T. Baker, C. T. Gibson, J. A. Campbell, D. A. Lewis, M. J. Jenkins, H. Willcock, J. M. Chalker and T. Hasell, *Chem. – Eur. J.*, 2019, **25**, 10433–10440.
14 K. Orme, A. H. Fistrovich and C. L. Jenkins, *Macromolecules*, 2020, **53**, 9353–9361.
15 T. S. Kleine, N. A. Nguyen, L. E. Anderson, S. Namnabat, E. A. LaVilla, S. A. Showghi, P. T. Dirlam, C. B. Arrington, M. S. Manchester, J. Schwiegerling, R. S. Glass, K. Char, R. A. Norwood, M. E. Mackay and J. Pyun, *ACS Macro Lett.*, 2016, **5**, 1152–1156.
16 P. Yan, W. Zhao, S. J. Tonkin, J. M. Chalker, T. L. Schiller and T. Hasell, *Chem. Mater.*, 2022, **34**, 1167–1178.
17 M. S. Karunarathna, C. P. Maladeniya, M. K. Lauer, A. G. Tennyson and R. C. Smith, *RSC Adv.*, 2023, **13**, 3234–3240.
18 M. K. Lauer, A. G. Tennyson and R. C. Smith, *ACS Appl. Polym. Mater.*, 2020, **2**, 3761–3765.
19 M. K. Lauer, A. G. Tennyson and R. C. Smith, *Mater. Adv.*, 2021, **2**, 2391–2397.
20 B. G. S. Guinati, P. Y. Sauceda Oloño, N. L. Kapuge Dona, K. M. Derr, S. K. Wijeyatunga, A. G. Tennyson and R. C. Smith, *RSC Sustainability*, 2024, **2**, 1819–1827.
21 A. Hoefling, D. T. Nguyen, Y. J. Lee, S.-W. Song and P. Theato, *Mater. Chem. Front.*, 2017, **1**, 1818–1822.
22 C. V. Lopez, A. D. Smith and R. C. Smith, *RSC Adv.*, 2022, **12**, 1535–1542.
23 A. D. Smith, A. G. Tennyson and R. C. Smith, *Sustain. Chem.*, 2020, **1**, 209–237.
24 C. V. Lopez, A. D. Smith and R. C. Smith, *Macromol. Chem. Phys.*, 2023, **224**, 2300233.
25 C. V. Lopez, K. M. Derr, A. D. Smith, A. G. Tennyson and R. C. Smith, *Chemistry*, 2023, **5**, 2166–2181.
26 C. Herrera, K. J. Ysinga and C. L. Jenkins, *ACS Appl. Mater. Interfaces*, 2019, **11**, 35312–35318.
27 A. D. Tikoalu, N. A. Lundquist and J. M. Chalker, *Adv. Sustainable Syst.*, 2020, **4**, 1900111.
28 C. V. Lopez, M. S. Karunarathna, M. K. Lauer, C. P. Maladeniya, T. Thiounn, E. D. Ackley and R. C. Smith, *J. Polym. Sci.*, 2020, **58**, 2259–2266.
29 A. E. Davis, K. B. Sayer and C. L. Jenkins, *Polym. Chem.*, 2022, **13**, 4634–4640.
30 F. Stojcevski, M. K. Stanfield, D. J. Hayne, M. Mann, N. A. Lundquist, J. M. Chalker and L. C. Henderson, *Sustainable Mater. Technol.*, 2022, **32**, e00400.
31 A. Gupta, M. J. H. Worthington, H. D. Patel, M. R. Johnston, M. Puri and J. M. Chalker, *ACS Sustainable Chem. Eng.*, 2022, **10**, 9022–9028.

32 I. Gomez, O. Leonet, J. A. Blazquez and D. Mecerreyes, *ChemSusChem*, 2016, **9**, 3419–3425.
33 B. Zhang, L. J. Dodd, P. Yan and T. Hasell, *React. Funct. Polym.*, 2021, **161**, 104865.
34 M. P. Crockett, A. M. Evans, M. J. H. Worthington, I. S. Albuquerque, A. D. Slattery, C. T. Gibson, J. A. Campbell, D. A. Lewis, G. J. L. Bernardes and J. M. Chalker, *Angew. Chem., Int. Ed.*, 2016, **55**, 1714–1718.
35 D. J. Parker, H. A. Jones, S. Petcher, L. Cervini, J. M. Griffin, R. Akhtar and T. Hasell, *J. Mater. Chem. A*, 2017, **5**, 11682–11692.
36 M. J. H. Worthington, R. L. Kucera, I. S. Albuquerque, C. T. Gibson, A. Sibley, A. D. Slattery, J. A. Campbell, S. F. K. Alboaiji, K. A. Muller, J. Young, N. Adamson, J. R. Gascooke, D. Jampaiah, Y. M. Sabri, S. K. Bhargava, S. J. Ippolito, D. A. Lewis, J. S. Quinton, A. V. Ellis, A. Johs, G. J. L. Bernardes and J. M. Chalker, *Chem. – Eur. J.*, 2017, **23**, 16219–16230.
37 N. A. Lundquist, M. J. H. Worthington, N. Adamson, C. T. Gibson, M. R. Johnston, A. V. Ellis and J. M. Chalker, *RSC Adv.*, 2018, **8**, 1232–1236.
38 K. B. Sayer, V. L. Miller, Z. Merrill, A. E. Davis and C. L. Jenkins, *Polym. Chem.*, 2023, **14**, 3091–3098.
39 M. E. Duarte, B. Huber, P. Theato and H. Mutlu, *Polym. Chem.*, 2020, **11**, 241–248.
40 N. L. Kapuge Dona, P. Y. Sauceda-Oloño and R. C. Smith, *J. Polym. Sci.*, 2024, **63**, 789–799.
41 C. P. Maladeniya, N. L. Kapuge Dona, A. D. Smith and R. C. Smith, *Macromol*, 2023, **3**, 681–692.
42 K. A. Tisdale, N. L. Kapuge Dona and R. C. Smith, *Molecules*, 2024, **29**, 4209.
43 M. S. Karunarathna, M. K. Lauer and R. C. Smith, *J. Mater. Chem. A*, 2020, **8**, 20318–20322.
44 N. L. Kapuge Dona, C. P. Maladeniya and R. C. Smith, *Eur. J. Org. Chem.*, 2024, **27**, e202301269.
45 K. A. Tisdale, N. L. Kapuge Dona, C. P. Maladeniya and R. C. Smith, *J. Polym. Environ.*, 2024, **32**, 4842–4854.
46 V. Hanna, M. Graysmark, H. Willcock and T. Hasell, *J. Mater. Chem. A*, 2024, **12**, 1211–1217.
47 P. Yan, W. Zhao, S. J. Tonkin, J. M. Chalker, T. L. Schiller and T. Hasell, *Chem. Mater.*, 2022, **34**, 1167–1178.
48 C. P. Maladeniya, M. S. Karunarathna, M. K. Lauer, C. V. Lopez, T. Thiounn and R. C. Smith, *Mater. Adv.*, 2020, **1**, 1665–1674.
49 J. J. Dale, V. Hanna and T. Hasell, *ACS Appl. Polym. Mater.*, 2023, **5**, 6761–6765.
50 T. Thiounn, M. S. Karunarathna, L. M. Slann, M. K. Lauer and R. C. Smith, *J. Polym. Sci.*, 2020, **58**, 2943–2950.
51 C. M. Hull, L. A. Weinland, S. R. Olsen and W. G. France, *Ind. Eng. Chem.*, 1948, **40**, 513–517.
52 Y. Nakamura, K. Mori and F. Akaishi, *Rubber Chem. Technol.*, 1977, **50**, 660–670.
53 K. Tsuchiya, K. Terada, Y. Tsuji, S. S. Y. Law, H. Masunaga, T. Katashima, T. Sakai and K. Numata, *Polym. J.*, 2024, **56**, 391–400.
54 K. Tamási and M. S. Kollár, *Int. J. Eng. Res. Sci. Technol.*, 2018, **4**, 28–37.
55 D. M. Beaupre and R. G. Weiss, *Molecules*, 2021, **26**, 3332.
56 J. J. Dale, S. Petcher and T. Hasell, *ACS Appl. Polym. Mater.*, 2022, **4**, 3169–3173.
57 J. J. Dale, J. Stanley, R. A. Dop, G. Chronowska-Bojczuk, A. J. Fielding, D. R. Neill and T. Hasell, *Eur. Polym. J.*, 2023, **195**, 112198.
58 S. M. Erhan and R. Kleiman, *J. Am. Oil Chem. Soc.*, 1993, **70**, 309–311.
59 R. Hodges, *Rubber Plast. Wkly.*, 1961, **21**, 666–668.
60 Y. Nakamura, K. Mori and T. Nakamura, *Rubber Chem. Technol.*, 1976, **49**, 1031.
61 Y. Nakamura, K. Mori and F. Akaishi, *Rubber Chem. Technol.*, 1977, **50**, 660.
62 Shore Hardness Durometer Chart and Comparisons, **https://hapcoincorporated.com/resources/hardness-chart/**, accessed January 24, 2025.
63 D. McClements, All About the Shore A Hardness Scale, **https://www.xometry.com/resources/materials/shore-a-hardness-scale/**, accessed January 24, 2025.

